

# The Pseudoscalar Meson and Heavy Vector Meson Scattering Lengths

Zhan-Wei Liu\*

*Department of Physics and State Key Laboratory of Nuclear Physics and Technology  
Peking University, Beijing 100871, China*

Yan-Rui Liu†

*Department of Physics, H-27, Tokyo Institute of Technology, Meguro, Tokyo 152-8551, Japan*

Xiang Liu‡

*School of Physical Science and Technology, Lanzhou University, Lanzhou 730000, China*

Shi-Lin Zhu§

*Department of Physics and State Key Laboratory of Nuclear Physics and Technology  
and Center of High Energy Physics, Peking University, Beijing 100871, China*

We have systematically studied the S-wave pseudoscalar meson and heavy vector meson scattering lengths to the third order with the chiral perturbation theory, which will be helpful to reveal their strong interaction. For comparison, we have presented the numerical results of the scattering lengths (1) in the framework of the heavy meson chiral perturbation theory and (2) in the framework of the infrared regularization. The chiral expansion converges well in some channels.

PACS numbers: 12.39.Fe, 14.40.Lb, 13.75.Lb

Keywords: Scattering length, heavy meson chiral perturbation theory, infrared regularization

## I. INTRODUCTION

In the past eight years we have witnessed the renaissance of the hadron spectroscopy. Many interesting new hadron states were discovered experimentally, some of which do not fit into the quark model easily. These new hadron states include (1) the famous XYZ states, which are either charmonium or charmonium-like states above the open-charm decay threshold; (2) the narrow charm-strange mesons  $D_{s0}(2317)$ ,  $D_{s1}(2460)$  etc.; (3) the charged Upsilon-like  $Z_b$  states recently announced by Belle collaboration [1]. A general feature of many of these new hadrons is that they are very close to the two open-flavor meson threshold. For example,  $X(3872)$  is very close to the  $\bar{D}D^*$ ,  $\rho J/\psi$  and  $\omega J/\psi$  threshold.  $D_{s0}(2317)$  is very close to the  $DK$  threshold. These charged  $Z_b$  states are very close to the  $\bar{B}^{(*)}B^*$  threshold. Because of their proximity to the two meson threshold, one may wonder whether some of these new hadron states are good candidates of loosely bound molecular states composed of two mesons? Or will the coupled-channel effect between the bare  $q\bar{q}$  state in the quark model and the two meson continuum help lower and push the mass of the bare quark model state close to the threshold? In order to allow the above two mechanisms work, there must exist attractive interaction between the two mesons.

Generally speaking, it is very difficult to study the hadron interaction starting from the first principle of strong interaction, i.e., quantum chromodynamics. Most of such investigations are performed on the lattice numerically. However, we may turn to chiral perturbation theory for help if one of the interacting mesons is a light pseudoscalar meson. In this case one can derive the scattering amplitude order by order rigorously. From the scattering amplitude, we can extract the scattering length, which is directly related to the hadron interaction. In this work we will study the pseudoscalar meson  $\phi$  and heavy vector meson  $D^*$  scattering lengths in order to learn whether there exists attraction between the pseudoscalar meson  $\phi$  and heavy vector meson  $D^*$ . Such a study will provide valuable information on their interaction to the  $D^*K$  system.

Up to now, a few new charmed mesons and their properties have attracted much interest over the past few years, especially the extremely narrow  $D_{s0}(2317)$ ,  $D_{s1}(2460)$  states. The  $D(D_s)$  and  $D^*(D_s^*)$  mesons constitute the lightest charmed doublet according to heavy quark symmetry. The recently observed new charmed particle  $D_{s0}(2317)$  is

---

\*Electronic address: liuzhanwei@pku.edu.cn

†Electronic address: yrliu@th.phys.titech.ac.jp

‡Electronic address: xiangliu@lzu.edu.cn

§Electronic address: zhushl@pku.edu.cn

speculated to be a candidate of possible molecular states composed of the  $D$  meson and  $K$  meson. The  $DK$  interaction is very important for us to understand the underlying structure of the  $D_{s0}(2317)$  meson [2, 3]. There have been some lattice investigations on the  $\pi D$  scattering [4–6],  $KD$  scattering and  $D_{s0}(2317)$  [7–9]. If there are strongly attractive interactions between them, the  $D^*$  meson and pseudoscalar meson might also form possible molecular states. Our present study of the  $\phi D^*$  scattering with chiral perturbation theory would be helpful to the future lattice simulation of the  $\phi D^*$  scattering numerically.

Chiral perturbation theory and lattice QCD are widely used to study the hadron interaction in the nonperturbative region of QCD [10–17]. The interaction between the  $D$  meson and the light pseudoscalar meson was studied recently with chiral perturbation theory [18–20]. It is interesting to extend the same formalism to study the interaction of the heavy vector meson  $D^*$  and the light pseudoscalar meson. In this paper, we will calculate the S-wave scattering lengths of the pseudoscalar meson and  $D^*$  meson with the heavy meson chiral perturbation theory (HM $\chi$ PT) and the infrared regularization (IR)[21–28]. The scattering length  $a_{\phi D^*}$  reflects their interaction. In our formalism  $a_{\phi D^*}$  is related to the threshold  $T$ -matrix  $T_{\phi D^*}$ :  $T_{\phi D^*} = 8\pi(1 + \frac{m_\phi}{M_{D^*}})a_{\phi D^*}$ , where  $m_\phi$  and  $M_{D^*}$  are the masses of the light pseudoscalar meson and  $D^*$  meson respectively.

With the explicit power counting scheme, HM $\chi$ PT is a useful tool to investigate the heavy meson interactions [21–24]. We will expand our calculation by  $\epsilon = p/\Lambda_\chi$ , where  $p$  represents the momentum of the light pseudoscalar meson, the small residue momentum of the heavy meson in the nonrelativistic limit, or the mass difference  $\delta$  between  $D$  and  $D^*$  mesons, and  $\Lambda_\chi$  represents either the chiral symmetry breaking scale around  $4\pi f_\pi$  or the heavy mesons' masses  $\bar{M}$  (about 1900 MeV) in the chiral and heavy quark symmetry limit. The IR scheme is also a useful tool based on chiral perturbation theory [25–28], which ensures both good power counting and correct analyticity. IR and HM $\chi$ PT generally lead to the same results except that the IR formalism includes the higher-order infrared parts of the loop graphs [25].

This paper is organized as follows. In Sec. II we list the basic notations, the relevant Lagrangians, and the chiral corrections to the threshold  $T$ -matrices with HM $\chi$ PT. We present the IR expressions in Sec. III. The low-energy constants (LECs) are estimated in Sec. IV. Finally, we give the numerical results and discussions in Sec. V.

## II. THE $T$ -MATRICES WITH THE HEAVY MESON CHIRAL PERTURBATION THEORY

We list the Lagrangian of HM $\chi$ PT at the leading order here,

$$\mathcal{L}_{\phi\phi}^{(2)} = f^2 \text{Tr} \left( u_\mu u^\mu + \frac{\chi_+}{4} \right), \quad (1)$$

$$\mathcal{L}_{H\phi}^{(1)} = -\langle (iv \cdot \partial H) \bar{H} \rangle + \langle H v \cdot \Gamma \bar{H} \rangle + g \langle H \not{v} \gamma_5 \bar{H} \rangle - \frac{1}{8} \delta \langle H \sigma^{\mu\nu} \bar{H} \sigma_{\mu\nu} \rangle, \quad (2)$$

where  $f$  is the decay constant of the pseudoscalar meson in the chiral limit, and

$$H = \frac{1+\not{v}}{2} (P_\mu^* \gamma^\mu + i P \gamma_5), \quad \bar{H} = \gamma^0 H^\dagger \gamma^0 = (P_\mu^{*\dagger} \gamma^\mu + i P^\dagger \gamma_5) \frac{1+\not{v}}{2}, \quad (3)$$

$$P = (D^0, D^+, D_s^+), \quad P_\mu^* = (D^{*0}, D^{*+}, D_s^{*+})_\mu. \quad (4)$$

Heavy quark symmetry is exact only when the heavy quark mass is infinite. In this work we will also systematically include effects of the explicitly broken heavy quark symmetry through the last term containing the  $D^*$  and  $D$  mass difference  $\delta$  in Eq. (2). The notations read

$$\Gamma_\mu = \frac{i}{2} [\xi^\dagger, \partial_\mu \xi], \quad u_\mu = \frac{i}{2} \{ \xi^\dagger, \partial_\mu \xi \}, \quad \xi = \exp(i\phi/2f), \quad \chi_\pm = \xi^\dagger \chi \xi^\dagger \pm \xi \chi \xi, \quad \chi = \text{diag}(m_\pi^2, m_\pi^2, 2m_K^2 - m_\pi^2), \quad (5)$$

$$\phi = \sqrt{2} \begin{pmatrix} \frac{\pi^0}{\sqrt{2}} + \frac{\eta}{\sqrt{6}} & \pi^+ & K^+ \\ \pi^- & -\frac{\pi^0}{\sqrt{2}} + \frac{\eta}{\sqrt{6}} & K^0 \\ K^- & \bar{K}^0 & -\frac{2}{\sqrt{6}}\eta \end{pmatrix}. \quad (6)$$

The following Lagrangians at the second and third order are used in the calculation of the threshold  $T$ -matrices,<sup>1</sup>

$$\mathcal{L}_{H\phi}^{(2)} = c_0 \langle H \bar{H} \rangle \text{Tr}(\chi_+) + c_1 \langle H \chi_+ \bar{H} \rangle - c_2 \langle H \bar{H} \rangle \text{Tr}(v \cdot u v \cdot u) - c_3 \langle H v \cdot u v \cdot u \bar{H} \rangle, \quad (7)$$

<sup>1</sup> The sign in front of  $c_1$  in Eq. (9) of Ref. [18] should be +. The signs in Eqs. (12) and (13) should be consequently changed.

$$\mathcal{L}_{H\phi}^{(3)} = \kappa_0 \delta \langle H \bar{H} \rangle \text{Tr}(\chi_+) + \kappa_1 \delta \langle H \chi_+ \bar{H} \rangle - \kappa_2 \delta \langle H \bar{H} \rangle \text{Tr}(v \cdot u \, v \cdot u) - \kappa_3 \delta \langle H v \cdot u \, v \cdot u \bar{H} \rangle + \kappa \langle H [\chi_-, v \cdot u] \bar{H} \rangle. \quad (8)$$

The  $O(\epsilon^2)$  and  $O(\epsilon^3)$  Lagrangians could also contain terms like  $\langle H \sigma^{\mu\nu} \bar{H} \sigma_{\mu\nu} \rangle \text{Tr}(\chi_+)$ ,  $\langle H \sigma^{\mu\nu} \chi_+ \bar{H} \sigma_{\mu\nu} \rangle$ . These terms break the heavy quark symmetry hence are suppressed. They lead to different LECs  $c_i$ 's and  $\kappa_i$ 's for the  $\phi D$  and  $\phi D^*$  scattering, although they do not result in the new independent vertices we need.

There are eleven independent  $T$ -matrices in the pseudoscalar meson and  $D^*$  meson scattering due to the isospin symmetry. The threshold  $T$ -matrices start at  $O(\epsilon)$ , which can be derived from Eq. (2)

$$\begin{aligned} T_{\pi D^*}^{(3/2)} &= -\frac{m_\pi}{f_\pi^2}, & T_{\pi D^*}^{(1/2)} &= \frac{2m_\pi}{f_\pi^2}, & T_{\pi D_s^*}^{(1)} &= 0, & T_{KD^*}^{(0)} &= \frac{2m_K}{f_K^2}, & T_{KD^*}^{(1)} &= 0, & T_{KD_s^*}^{(1/2)} &= -\frac{m_K}{f_K^2}, \\ T_{\bar{K}D^*}^{(1)} &= -\frac{m_K}{f_K^2}, & T_{\bar{K}D^*}^{(0)} &= \frac{m_K}{f_K^2}, & T_{\bar{K}D_s^*}^{(1/2)} &= \frac{m_K}{f_K^2}, & T_{\eta D^*}^{(1/2)} &= 0, & T_{\eta D_s^*}^{(0)} &= 0, \end{aligned} \quad (9)$$

where the superscript in the bracket represents the total isospin of the channel. We express  $T$ -matrices with the renormalized decay constants  $f_\pi$ ,  $f_K$  and  $f_\eta$  [29, 30] rather than  $f$  here. The difference could be accounted for through  $T$ -matrices at  $O(\epsilon^3)$  or higher order.

Similarly we get the results at  $O(\epsilon^2)$ ,<sup>2</sup>

$$\begin{aligned} T_{\pi D^*}^{(3/2)} &= \frac{8c_0 m_\pi^2 + 4c_1 m_\pi^2 + 2c_2 m_\pi^2 + c_3 m_\pi^2}{f_\pi^2}, & T_{\pi D^*}^{(1/2)} &= \frac{8c_0 m_\pi^2 + 4c_1 m_\pi^2 + 2c_2 m_\pi^2 + c_3 m_\pi^2}{f_\pi^2}, \\ T_{\pi D_s^*}^{(1)} &= \frac{8c_0 m_\pi^2 + 2c_2 m_\pi^2}{f_\pi^2}, & T_{KD^*}^{(0)} &= \frac{8c_0 m_K^2 + 8c_1 m_K^2 + 2c_2 m_K^2 + 2c_3 m_K^2}{f_K^2}, & T_{KD^*}^{(1)} &= \frac{8c_0 m_K^2 + 2c_2 m_K^2}{f_K^2}, \\ T_{KD_s^*}^{(1/2)} &= \frac{8c_0 m_K^2 + 4c_1 m_K^2 + 2c_2 m_K^2 + c_3 m_K^2}{f_K^2}, & T_{\bar{K}D^*}^{(1)} &= \frac{8c_0 m_K^2 + 4c_1 m_K^2 + 2c_2 m_K^2 + c_3 m_K^2}{f_K^2}, \\ T_{\bar{K}D^*}^{(0)} &= \frac{8c_0 m_K^2 - 4c_1 m_K^2 + 2c_2 m_K^2 - c_3 m_K^2}{f_K^2}, & T_{\bar{K}D_s^*}^{(1/2)} &= \frac{8c_0 m_K^2 + 4c_1 m_K^2 + 2c_2 m_K^2 + c_3 m_K^2}{f_K^2}, \\ T_{\eta D^*}^{(1/2)} &= \frac{24c_0 m_\eta^2 + 4c_1 m_\pi^2 + 6c_2 m_\eta^2 + c_3 m_\eta^2}{3f_\eta^2}, & T_{\eta D_s^*}^{(0)} &= \frac{24c_0 m_\eta^2 + 32c_1 m_K^2 - 16c_1 m_\pi^2 + 6c_2 m_\eta^2 + 4c_3 m_\eta^2}{3f_\eta^2}. \end{aligned} \quad (10)$$

Here we have used the Gell-Mann-Okubo mass relation  $m_\eta^2 = (4m_K^2 - m_\pi^2)/3$ , which makes the expressions more concise.

The  $T$ -matrices contain contributions from both the tree and loop diagrams. We show all eighteen loop diagrams which contribute to the threshold  $T$ -matrix at  $O(\epsilon^3)$  in Fig. 1. We calculate them with the dimensional regularization and modified minimal subtraction. More specifically, for the unstable  $D^*$  meson we renormalize its wave function at the point  $\bar{r}$

$$Z_{D^*} = 1 + \left. \frac{d\Pi_{D^*}(r)}{d(r)} \right|_{r=\bar{r}}, \quad (11)$$

where  $\Pi_{D^*}(r)$  is the one-particle irreducible  $D^*$  self-energy,  $r$  is the remaining momentum  $r \equiv v \cdot p - \hat{M}$ , and  $\bar{r}$  is the complex pole of the propagator  $\bar{r} - \delta - \Pi_{D^*}(\bar{r}) = 0$ . The divergences from loops can be absorbed after the wave function renormalization and redefinitions of  $\kappa_i$ ,

$$4\kappa_0 + \kappa_2 = \frac{2g^2 L}{9f^2} + 4\kappa_0^r + \kappa_2^r, \quad \kappa_1 = \frac{5g^2 L}{12f^2} + \kappa_1^r, \quad \kappa_3 = -\frac{3g^2 L}{f^2} + \kappa_3^r, \quad \kappa = \frac{3L}{4f^2} + \kappa^r, \quad (12)$$

where

$$L = \frac{\lambda^{D-4}}{16\pi^2} \left\{ \frac{1}{D-4} + \frac{1}{2}(\gamma_E - 1 - \ln 4\pi) \right\}. \quad (\text{Euler constant } \gamma_E = 0.5772157) \quad (13)$$

Here  $\lambda$  is the scale of the dimensional regularization. We will set it at  $4\pi f_\pi$ ,  $4\pi f_K$  and  $4\pi f_\eta$  respectively for the pion-, kaon- and  $\eta$ -scattering.

---

<sup>2</sup> The constant  $C_1$  in  $T_{DK}^{(0)}$  of Ref. [18] should be  $\frac{1}{2}(3C_1 - C_0)$ . The corrected  $T$ -matrix is the same as  $T_{KD^*}^{(0)}$  here.

In order to make the expressions short, we introduce the following notations and functions:

$$\begin{aligned}
J &= -\frac{g^2}{24\pi^2(m_\eta^2 - m_\pi^2)f^4} \left( 2\pi m_\eta^3 + 2(m_\eta^2 - \delta^2)^{3/2} \cos^{-1}\left(-\frac{\delta}{m_\eta}\right) + 3m_\eta^2 \delta \log \frac{m_\eta}{\lambda} - 2m_\eta^2 \delta \right. \\
&\quad \left. - 2\delta^3 \log \frac{m_\eta}{\lambda} - 2\pi m_\pi^3 - 2(\delta^2 - m_\pi^2)^{3/2} \log \frac{m_\pi}{\lambda} + 2(\delta^2 - m_\pi^2)^{3/2} \log \frac{\sqrt{\delta^2 - m_\pi^2} + \delta}{\lambda} \right. \\
&\quad \left. - 2i\pi\delta^2 \sqrt{\delta^2 - m_\pi^2} + 2i\pi m_\pi^2 \sqrt{\delta^2 - m_\pi^2} - 3m_\pi^2 \delta \log \frac{m_\pi}{\lambda} + 2m_\pi^2 \delta + 2\delta^3 \log \frac{m_\pi}{\lambda} \right), \\
W(m) &= -\frac{g^2}{16\pi^2 f^4} \begin{cases} 2\sqrt{m^2 - \delta^2} \cos^{-1}\left(-\frac{\delta}{m}\right) + 2\delta \log\left(\frac{m}{\lambda}\right) + 2\pi m - \delta & m > \delta \\ 2\delta \log \frac{m}{\lambda} + 2\sqrt{\delta^2 - m^2} \left( \log \frac{\sqrt{\delta^2 - m^2} + \delta}{m} - i\pi \right) + 2\pi m - \delta & m \leq \delta \end{cases}, \\
V(m, \omega) &= \frac{\omega^3 \log \frac{m}{\lambda}}{\pi^2 f^4} - \frac{\omega^3}{2\pi^2 f^4} - \frac{\omega^2}{\pi^2 f^4} \begin{cases} -\sqrt{m^2 - \omega^2} \cos^{-1}\left(-\frac{\omega}{m}\right) & m^2 \geq \omega^2 \\ \sqrt{\omega^2 - m^2} \log \frac{\sqrt{\omega^2 - m^2} - \omega}{m} & m^2 < \omega^2, \omega < 0 \\ \sqrt{\omega^2 - m^2} \left( -\log \frac{\sqrt{\omega^2 - m^2} + \omega}{m} + i\pi \right) & m^2 < \omega^2, \omega \geq 0 \end{cases}. \quad (14)
\end{aligned}$$

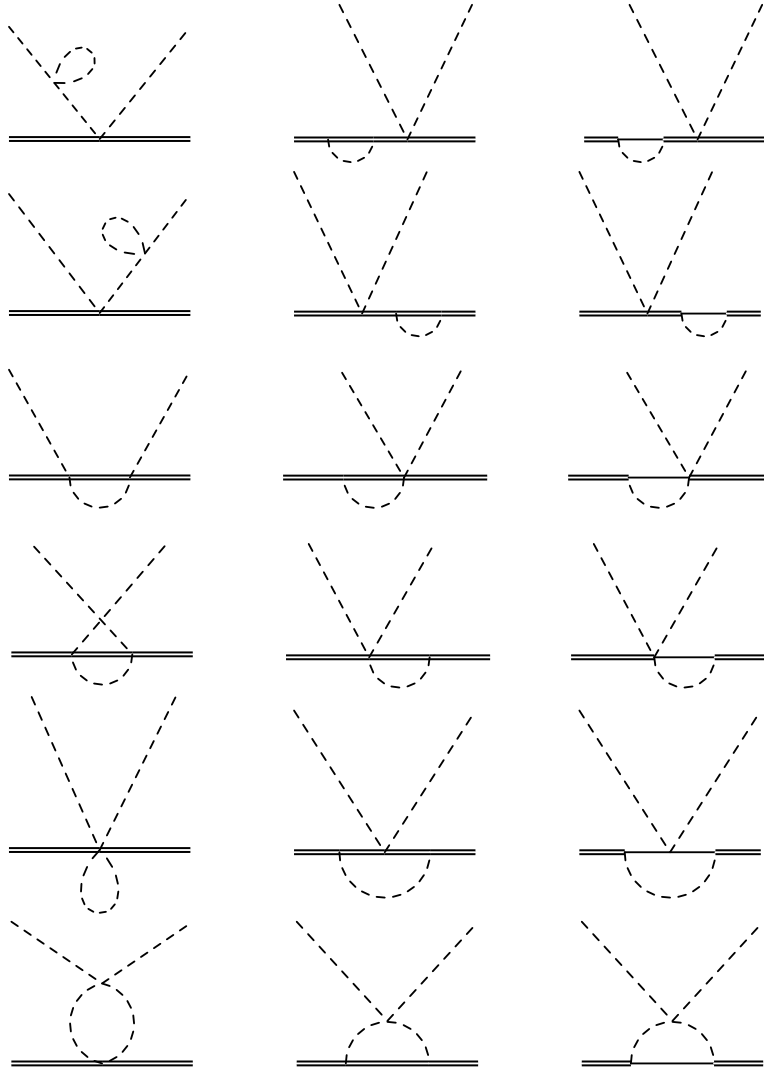


FIG. 1: Nonvanishing loop diagrams for the pseudoscalar meson and  $D^*$  meson scattering lengths to  $O(\epsilon^3)$  with HM $\chi$ PT and IR. The dashed lines, thin solid lines and thick solid lines represent the pseudoscalar Goldstone bosons,  $D$  mesons and  $D^*$  mesons, respectively.

In the third-order  $T$ -matrices there are some terms proportional to those in Eq. (10). Therefore, we divide the

$T$ -matrices into two parts,

$$T = \tilde{T} + T_2, \quad (15)$$

where  $T_2$  can be obtained from Eq. (10) through the following replacement:

$$c_0 \rightarrow \kappa_0^T \delta, \quad c_1 \rightarrow \kappa_1^T \delta, \quad c_2 \rightarrow \kappa_2^T \delta, \quad c_3 \rightarrow \kappa_3^T \delta. \quad (16)$$

The remaining  $\tilde{T}$  at  $O(\epsilon^3)$  reads

$$\begin{aligned} \tilde{T}_{\pi D^*}^{(3/2)} &= -\frac{1}{8}V(m_K, -m_\pi) - \frac{3}{8}V(m_\pi, -m_\pi) - \frac{1}{8}V(m_\pi, m_\pi) + \frac{1}{18}m_\pi^2 W(m_\eta) - \frac{1}{2}m_\pi^2 W(m_\pi) + 2V_1 - \frac{8m_\pi^3 \kappa^r}{f_\pi^2}, \\ \tilde{T}_{\pi D^*}^{(1/2)} &= \frac{1}{16}V(m_K, -m_\pi) - \frac{3}{16}V(m_K, m_\pi) - \frac{1}{2}V(m_\pi, m_\pi) + \frac{1}{18}m_\pi^2 W(m_\eta) - \frac{1}{2}m_\pi^2 W(m_\pi) - 4V_1 + \frac{16m_\pi^3 \kappa^r}{f_\pi^2}, \\ \tilde{T}_{\pi D_s^*}^{(1)} &= -\frac{1}{8}V(m_K, -m_\pi) - \frac{1}{8}V(m_K, m_\pi) + \frac{2}{9}m_\pi^2 W(m_\eta), \\ \tilde{T}_{KD^*}^{(0)} &= -\frac{3}{8}V(m_\eta, m_K) - \frac{1}{8}V(m_K, -m_K) - \frac{1}{2}V(m_K, m_K) - Jm_K^2 - \frac{1}{9}m_K^2 W(m_\eta) - 3V_2 - 3V_3 + V_4 + \frac{16m_K^3 \kappa^r}{f_K^2}, \\ \tilde{T}_{KD^*}^{(1)} &= -\frac{1}{8}V(m_\pi, m_K) - \frac{1}{8}V(m_K, -m_K) + \frac{Jm_K^2}{3} - \frac{1}{9}m_K^2 W(m_\eta) - V_2 + V_3 + \frac{V_4}{3}, \\ \tilde{T}_{KD_s^*}^{(1/2)} &= -\frac{3}{16}V(m_\eta, -m_K) - \frac{3}{16}V(m_\pi, -m_K) - \frac{1}{8}V(m_K, -m_K) - \frac{1}{8}V(m_K, m_K) - \frac{4}{9}m_K^2 W(m_\eta) + 3V_2 - \frac{8m_K^3 \kappa^r}{f_K^2}, \\ \tilde{T}_{KD^*}^{(1)} &= -\frac{3}{16}V(m_\eta, -m_K) - \frac{1}{16}V(m_\pi, -m_K) - \frac{1}{4}V(m_K, -m_K) - \frac{1}{8}V(m_K, m_K) - \frac{Jm_K^2}{3} - \frac{1}{9}m_K^2 W(m_\eta) \\ &\quad + 2V_2 + V_3 - \frac{2V_4}{3} - \frac{8m_K^3 \kappa^r}{f_K^2}, \\ \tilde{T}_{KD^*}^{(0)} &= \frac{3}{16}V(m_\eta, -m_K) - \frac{3}{16}V(m_\pi, -m_K) + \frac{1}{4}V(m_K, -m_K) - \frac{1}{8}V(m_K, m_K) + Jm_K^2 - \frac{1}{9}m_K^2 W(m_\eta) - 3V_3 \\ &\quad + \frac{8m_K^3 \kappa^r}{f_K^2}, \\ \tilde{T}_{KD_s^*}^{(1/2)} &= -\frac{3}{16}V(m_\eta, m_K) - \frac{3}{16}V(m_\pi, m_K) - \frac{1}{8}V(m_K, -m_K) - \frac{1}{8}V(m_K, m_K) - \frac{4}{9}m_K^2 W(m_\eta) - 3V_2 + \frac{8m_K^3 \kappa^r}{f_K^2}, \\ \tilde{T}_{\eta D^*}^{(1/2)} &= -\frac{3}{16}V(m_K, -m_\eta) - \frac{3}{16}V(m_K, m_\eta) - \frac{2}{3}m_K^2 W(m_K) + \frac{2}{9}m_\eta^2 W(m_\eta) - \frac{1}{18}m_\pi^2 W(m_\eta) + \frac{1}{2}m_\pi^2 W(m_\pi), \\ \tilde{T}_{\eta D_s^*}^{(0)} &= -\frac{3}{8}V(m_K, -m_\eta) - \frac{3}{8}V(m_K, m_\eta) - \frac{4}{3}m_K^2 W(m_K) + \frac{8}{9}m_\eta^2 W(m_\eta) - \frac{2}{9}m_\pi^2 W(m_\eta), \end{aligned} \quad (17)$$

where  $V_1 = V_2 = V_3 = V_4 = 0$  with HM $\chi$ PT but nonzero with IR.

The  $T$ -matrices of the pseudoscalar meson  $\phi$  and  $D$  meson scattering with HM $\chi$ PT were derived in Ref. [18]. For the  $\phi D$  case, there is no  $\phi DD$ -vertex in the leading order. Therefore in the loop calculation there are no similar diagrams of the third column in Fig. 1 where  $\phi D$  are the intermediate states. If we let  $\delta \rightarrow 0$  and neglect the explicit breaking of heavy quark symmetry, the  $T$ -matrices of the pseudoscalar meson and  $D^*$  scattering will be the same as those of the pseudoscalar meson and  $D$  meson scattering to  $O(\epsilon^3)$  at the threshold [18], which is required by the heavy quark symmetry.

### III. THE $T$ -MATRICES WITH THE INFRARED REGULARIZATION METHOD

For the IR scheme, we use the heavy meson Lagrangian with the relativistic form at the leading order,

$$\begin{aligned} \mathcal{L}_{H\phi}^{(1)} &= \mathcal{D}_\mu \tilde{P} \mathcal{D}^\mu \tilde{P}^\dagger - \dot{M}^2 \tilde{P} \tilde{P}^\dagger - \mathcal{D}_\mu \tilde{P}^{*\nu} \mathcal{D}^\mu \tilde{P}_\nu^{*\dagger} + (\dot{M} + \delta)^2 \tilde{P}^{*\nu} \tilde{P}_\nu^{*\dagger} \\ &\quad + i2g\dot{M}(\tilde{P}_\mu^* u^\mu \tilde{P}^\dagger - \tilde{P} u^\mu \tilde{P}_\mu^{*\dagger}) + g(\tilde{P}_\mu^* u_\alpha \mathcal{D}_\beta \tilde{P}_\nu^{*\dagger} - \mathcal{D}_\beta \tilde{P}_\mu^* u_\alpha \tilde{P}_\nu^{*\dagger}) \epsilon^{\mu\nu\alpha\beta}, \end{aligned} \quad (18)$$

where heavy quark symmetry is also assumed to relate the couplings of the  $\pi D^* D$ -vertex and  $\pi D^* D^*$ -vertex, and

$$\tilde{P} = \frac{P}{\sqrt{M}}, \quad i\mathcal{D}_\mu \tilde{P}_a = i\partial_\mu \tilde{P}_a - \Gamma_\mu^{ba} \tilde{P}_b, \quad i\mathcal{D}_\mu \tilde{P}_a^\dagger = i\partial_\mu \tilde{P}_a^\dagger + \Gamma_\mu^{ab} \tilde{P}_b^\dagger. \quad (\text{Similar for } \tilde{P}^*.) \quad (19)$$

The second-order and third-order Lagrangians we use are the same as the relevant terms in Eqs. (7, 8), but some coefficients should be redefined to fit the experimental data,

$$\mathcal{L}_{H\phi}^{(2)} = 2\dot{M}(c_0\tilde{P}^{*\mu}\tilde{P}_\mu^{*\dagger}\text{Tr}(\chi_+) + c_1\tilde{P}^{*\mu}\chi_+\tilde{P}_\mu^{*\dagger} - c_2\tilde{P}^{*\mu}\tilde{P}_\mu^{*\dagger}\text{Tr}(u \cdot u) - c_3\tilde{P}^{*\mu}u \cdot u\tilde{P}_\mu^{*\dagger}), \quad (20)$$

$$\begin{aligned} \mathcal{L}_{H\phi}^{(3)} = & 2\dot{M}(\kappa_0\tilde{P}^{*\mu}\tilde{P}_\mu^{*\dagger}\text{Tr}(\chi_+)\delta + \kappa_1\tilde{P}^{*\mu}\chi_+\tilde{P}_\mu^{*\dagger}\delta - \kappa_2\tilde{P}^{*\mu}\tilde{P}_\mu^{*\dagger}\text{Tr}(u \cdot u)\delta - \kappa_3\tilde{P}^{*\mu}u \cdot u\tilde{P}_\mu^{*\dagger}\delta) \\ & + i\dot{M}\kappa \left( \mathcal{D}_\nu\tilde{P}^{*\mu}[\chi_-, u^\nu]\tilde{P}_\mu^{*\dagger} - \tilde{P}^{*\mu}[\chi_-, u^\nu]\mathcal{D}_\nu\tilde{P}_\mu^{*\dagger} \right). \end{aligned} \quad (21)$$

The  $T$ -matrices are nearly the same as those of  $\text{HM}\chi\text{PT}$  except that the expressions of  $J$ ,  $W(m)$ ,  $V(m, \omega)$ ,  $V_1$ ,  $V_2$ ,  $V_3$ , and  $V_4$  are more complicated. We list their definitions in the infrared scheme in Eq. (B7) in the Appendix. We have also verified that the results with IR are the same as those with  $\text{HM}\chi\text{PT}$  when  $\dot{M}$  approaches to infinity.

#### IV. LOW-ENERGY CONSTANTS

The difference of our results between  $\text{HM}\chi\text{PT}$  and IR originates at the third order due to different loop integrals. We use the same LECs at the first and second order for both  $\text{HM}\chi\text{PT}$  and IR. At the leading order, we have [31]

$$\begin{aligned} m_\pi &= 139 \text{ MeV}, \quad m_K = 494 \text{ MeV}, \quad \delta = 142 \text{ MeV}, \\ f_\pi &= 92 \text{ MeV}, \quad f_K = 113 \text{ MeV}, \quad f_\eta = 1.2f_K, \quad g = 0.59. \end{aligned}$$

At the second order, from the mass splitting between heavy mesons we get<sup>3</sup>

$$c_1 = \frac{1}{16} \frac{M_{D_s}^2 - M_D^2 + M_{D_s^*}^2 - M_{D^*}^2}{\dot{M}(m_K^2 - m_\pi^2)} = 0.12 \text{ GeV}^{-1}. \quad (22)$$

In order to obtain other LECs that can not be determined from the available experimental data, we resort to the resonance saturation model [32, 33].

At  $O(\epsilon^2)$  only the light unflavored mesons with  $J^P = 0^+$  and charmed mesons with  $J^P = 1^+$  contribute to the  $\phi\phi D^* D^*$  vertex at threshold. Thus we consider the scalar singlet  $\sigma(\sigma(600))$ , the scalar octet  $\kappa(\kappa(800), a_0(980), f_0(980))$ , and  $D_{s1}(2460)$  vector triplet in this section. In the Appendix A we will discuss the uncertainty of the LECs at this order.

Here we list the corresponding effective Lagrangians,

$$\begin{aligned} \mathcal{L}_{\sigma\pi\pi} &= 4\tilde{c}_d\text{Tr}(u \cdot u)\sigma + \tilde{c}_m\text{Tr}(\chi_+)\sigma, \\ \mathcal{L}_{\sigma P^* P^*} &= c_\sigma P^{*\mu} P_\mu^{*\dagger} \sigma. \end{aligned} \quad (23)$$

Integrating the  $\sigma$  meson out through the t-channel we get

$$\mathcal{L}_{\text{eff}}^\sigma \sim \frac{2c_\sigma\tilde{c}_m}{m_\sigma^2}\text{Tr}(\chi_+)P^{*\mu}P_\mu^{*\dagger} + \frac{8c_\sigma\tilde{c}_d}{m_\sigma^2}\text{Tr}(v \cdot u v \cdot u)P^{*\mu}P_\mu^{*\dagger} \quad (24)$$

Similarly, from the Lagrangians of the scalar octet  $\kappa$

$$\begin{aligned} \mathcal{L}_{\kappa\pi\pi} &= 4c_d\text{Tr}(u \cdot u\kappa) + c_m\text{Tr}(\chi_+\kappa), \\ \mathcal{L}_{\kappa P^* P^*} &= c_\kappa P^{*\mu} \kappa P_\mu^{*\dagger}, \end{aligned} \quad (25)$$

one obtains

$$\mathcal{L}_{\text{eff}}^\kappa \sim -\frac{2c_\kappa c_m}{3m_\kappa^2}\text{Tr}(\chi_+)P^{*\mu}P_\mu^{*\dagger} + \frac{2c_\kappa c_m}{m_\kappa^2}P^{*\mu}\chi_+P_\mu^{*\dagger} - \frac{8c_\kappa c_d}{3m_\kappa^2}\text{Tr}(v \cdot u v \cdot u)P^{*\mu}P_\mu^{*\dagger} + \frac{8c_\kappa c_d}{m_\kappa^2}P^{*\mu}v \cdot u v \cdot u P_\mu^{*\dagger} \quad (26)$$

Integrating  $D_{s1}(2460)$  out of the following interacting Lagrangian,

$$\mathcal{L}_{D_{s1}(2460)} = G_1 \left( D_{s1}^{\mu\dagger}(2460)u_\nu i\partial^\nu \tilde{P}_\mu^* - i\partial^\nu \tilde{P}_\mu^{*\dagger}u_\nu D_{s1}^\mu(2460) \right) + G_2 \left( -i\partial_\nu D_{s1}^{\mu\dagger}(2460)u_\nu \tilde{P}_\mu^* + \tilde{P}_\mu^*u_\nu i\partial_\nu D_{s1}^\mu(2460) \right)$$

---

<sup>3</sup> The coefficient 4 in Eq. (33) of Ref. [18] should be 8. The correct values of  $c_1$  are  $0.12 \text{ GeV}^{-1}$  in Eq. (22) and  $0.10 \text{ GeV}^{-1}$  in Eq. (36) of this paper.

$$= (G_1 + G_2) \left( D_{s1}^{\mu\dagger}(2460) u_\nu i \partial^\nu \tilde{P}_\mu^* - i \partial^\nu \tilde{P}_\mu^{*\dagger} u_\nu D_{s1}^\mu(2460) \right) + O(\epsilon^2), \quad (27)$$

one gets

$$\mathcal{L}_{\text{eff}}^{D_{s1}(2460)} = -\frac{|G_1 + G_2|^2 M_{D^*}}{M_{D_{s1}(2460)}^2 - M_{D^*}^2} P^{*\mu} v \cdot u \, v \cdot u P_\mu^{*\dagger}. \quad (28)$$

The effective coupling constants  $|G_1 + G_2|$  were estimated with QCD sum rule approach in Ref. [34]:  $|G_1 + G_2| = 1.2 \pm 0.2$ .

Adding the above effective Lagrangians (24), (26) and (28) together, one can estimate the LECs by comparing the sum with the relevant terms in Eq. (7),

$$c_0 = \frac{c_\sigma \tilde{c}_m}{m_\sigma^2} - \frac{c_\kappa c_m}{3m_\kappa^2}, \quad c_1 = \frac{c_\kappa c_m}{m_\kappa^2}, \quad c_2 = -\frac{4c_\sigma \tilde{c}_d}{m_\sigma^2} + \frac{4c_\kappa c_d}{3m_\kappa^2}, \quad c_3 = -\frac{4c_\kappa c_d}{m_\kappa^2} + \frac{|G_1 + G_2|^2 M_{D^*}}{2(M_{D_{s1}(2460)}^2 - M_{D^*}^2)}. \quad (29)$$

For the broad resonances  $\sigma(600)$  and  $\kappa(800)$ , we use the masses and widths extracted from a model-independent way [35, 36],

$$m_\sigma = 441_{-8}^{+16} \text{ MeV}, \quad \Gamma_\sigma = 544_{-25}^{+18} \text{ MeV}; \quad m_{\kappa(800)} = 658 \pm 13 \text{ MeV}, \quad \Gamma_{\kappa(800)} = 557 \pm 24 \text{ MeV}. \quad (30)$$

In our numerical analysis, we take  $m_\kappa = 820 \text{ MeV}$  for illustration.

For the coupling constants  $c_d$  and  $c_m$ , we use [32]

$$|c_d| = 3.2 \times 10^{-2} \text{ GeV}, \quad |c_m| = 4.2 \times 10^{-2} \text{ GeV}, \quad c_d c_m > 0. \quad (31)$$

Although there is no empirical value of  $c_\kappa$ , we may get it by comparing the  $c_1$ 's obtained in different ways in Eq. (22) and Eq. (29)

$$|c_\kappa| = 1.9, \quad c_\kappa c_m > 0. \quad (32)$$

Moreover the coupling constants should obey the nonet relations in the large  $N_c$  limit,

$$\tilde{c}_d = \frac{\zeta}{\sqrt{3}} c_d, \quad \tilde{c}_m = \frac{\zeta}{\sqrt{3}} c_m, \quad c_\sigma = \frac{\zeta}{\sqrt{3}} c_\kappa, \quad \zeta = \pm 1. \quad (33)$$

In this way, we get the LECs at  $O(\epsilon^2)$ ,

$$c_0 = 0.10 \text{ GeV}^{-1}, \quad c_1 = 0.12 \text{ GeV}^{-1}, \quad c_2 = -0.30 \text{ GeV}^{-1}, \quad c_3 = 0.42 \text{ GeV}^{-1}. \quad (34)$$

The resonance saturation method may bring large uncertainty in the determination of the LECs at the third order. We take the value of  $\kappa^r$  in Ref [18]

$$\kappa^r = -0.33 \text{ GeV}^{-2}, \quad (35)$$

which is obtained by fitting the lattice QCD results [37]. We simply assume the other tree diagram contributions at  $O(\epsilon^3)$  are small and neglect them as done in Refs. [12, 38].

## V. NUMERICAL RESULTS AND DISCUSSIONS

We show the numerical results of the  $T$ -matrices order by order and the scattering lengths with HM $\chi$ PT in Table I<sup>4</sup>. The positive real parts of  $a_{\pi D^*}^{(1/2)}$ ,  $a_{K D^*}^{(0)}$ ,  $a_{\bar{K} D^*}^{(0)}$ ,  $a_{\bar{K} D_s^*}^{(1/2)}$ ,  $a_{\eta D^*}^{(1/2)}$  and  $a_{\eta D_s^*}^{(0)}$  indicate that the interactions are attractive

---

<sup>4</sup> The numerical values in Ref. [18] also need a few corrections. The corrections are given here in the form of  $\{\mathcal{O}(p^2), \text{Total}, \text{Scattering lengths}\}_T$ . In Table I, they are  $\{-14.2, 1.1, 0.04\}_{T^{(0)}}$ ,  $\{6.4, 7.5 + 5.5i, 0.23 + 0.17i\}_{T_{D\eta}}$ , and  $\{-6.7, -6.2 + 11.1i, -0.19 + 0.35i\}_{T_{D_s\eta}}$ . In Table II, they are  $\{-14.2, 0.5, 0.02\}_{T^{(0)}}$ ,  $\{6.4, 7.3 + 5.5i, 0.26 + 0.20i\}_{T_{B\eta}}$ , and  $\{-6.9, -6.6 + 11.1i, -0.24 + 0.35i\}_{T_{B_s\eta}}$ . In Table III, they are  $\{-15.1, -0.6, -0.02\}_{T_{DK}^{(0)}}$ ,  $\{6.1, 7.3 + 5.5i, 0.22 + 0.17i\}_{T_{D\eta}}$ , and  $\{-7.4, -7.0 + 11.1i, -0.22 + 0.35i\}_{T_{D_s\eta}}$ . To get a positive  $a_{D_s\eta}$  and nearly vanishing  $a_{D_s\pi}$ , one requires  $C_1 > 0.8 \text{ GeV}^{-1}$  and  $C_0 < 4.2 \text{ GeV}^{-1}$ .

TABLE I: The threshold  $T$ -matrices for the pseudoscalar meson and  $D^*$  meson scattering order by order in units of fm with HM $\chi$ PT.

	$O(\epsilon^1)$ $O(\epsilon^2)$		$O(\epsilon^3)$			Total	Scattering length
			loop	tree	total		
$T_{\pi D^*}^{(3/2)}$	-3.2	0.5	-1.-0.0096i	0.17	-0.88-0.0096i	-3.6-0.0096i	-0.13-0.00036i
$T_{\pi D^*}^{(1/2)}$	6.5	0.5	0.53-0.0096i	-0.33	0.19-0.0096i	7.1-0.0096i	0.27-0.00036i
$T_{\pi D_s^*}^{(1)}$	0	0.09	-1.1	0	-1.1	-1	-0.039
$T_{KD^*}^{(0)}$	15	7.5	11.-0.00016i	-9.8	1.1-0.00016i	24.-0.00016i	$0.76-5.2 \times 10^{-6}i$
$T_{KD^*}^{(1)}$	0	0.75	-1.5+5.6i	0	-1.5+5.6i	-0.7+5.6i	-0.022+0.18i
$T_{KD_s^*}^{(1/2)}$	-7.6	4.1	-5.9	4.9	-0.98	-4.5	-0.14
$T_{\bar{K}D^*}^{(1)}$	-7.6	4.1	-7.4-0.000054i	4.9	-2.5-0.000054i	-5.9-0.000054i	$-0.19-1.7 \times 10^{-6}i$
$T_{\bar{K}D^*}^{(0)}$	7.6	-2.6	8.8+0.00016i	-4.9	3.9+0.00016i	8.9+0.00016i	$0.29+5.2 \times 10^{-6}i$
$T_{\bar{K}D_s^*}^{(1/2)}$	7.6	4.1	4.+8.3i	-4.9	-0.86+8.3i	11.+8.3i	0.35+0.27i
$T_{\eta D^*}^{(1/2)}$	0	1.2	0.46+3.i	0	0.46+3.i	1.7+3.i	0.051+0.094i
$T_{\eta D_s^*}^{(0)}$	0	5.8	0.0036+6.1i	0	0.0036+6.1i	5.8+6.1i	0.18+0.19i

TABLE II: Comparison of the  $T$ -matrices from the loop diagrams for the pseudoscalar meson and  $D^*$  meson scattering between HM $\chi$ PT and IR.

	Intermediate state: $D$ meson				Intermediate state: $D^*$ meson				Loop: total	
	HM $\chi$ PT		IR		HM $\chi$ PT		IR		HM $\chi$ PT	IR
	$\delta = 142$ MeV	$\delta \rightarrow 0$	$\delta = 142$ MeV	$\delta \rightarrow 0$	$\delta = 142$ MeV	$\delta = 142$ MeV	$\delta = 142$ MeV	$\delta = 142$ MeV	$\delta = 142$ MeV	$\delta = 142$ MeV
$T_{\pi D^*}^{(3/2)}$	-0.053-0.0096i	0.014	-0.043-0.0076i	0.0045	-0.99	-0.84	-1.-0.0096i	-0.88-0.0076i		
$T_{\pi D^*}^{(1/2)}$	-0.053-0.0096i	0.014	-0.05-0.0093i	0.031	0.58	0.3	0.53-0.0096i	0.25-0.0093i		
$T_{\pi D_s^*}^{(1)}$	-0.043	-0.046	-0.03	-0.04	-1.1	-0.88	-1.1	-0.91		
$T_{KD^*}^{(0)}$	0.69-0.00016i	0.93	0.46-0.00015i	0.76	10.	7.5	11.-0.00016i	8.-0.00015i		
$T_{KD^*}^{(1)}$	-0.076+0.000054i	-0.14	-0.014+0.0019i	-0.18	-1.4+5.6i	-3.6+2.9i	-1.5+5.6i	-3.6+2.9i		
$T_{KD_s^*}^{(1/2)}$	0.46	0.51	0.29	0.43	-6.3	-13.	-5.9	-13.		
$T_{\bar{K}D^*}^{(1)}$	0.31-0.000054i	0.4	0.17-0.00099i	0.38	-7.7	-14.	-7.4-0.000054i	-14.-0.00099i		
$T_{\bar{K}D^*}^{(0)}$	-0.46+0.00016i	-0.68	-0.33-0.0027i	-0.51	9.3	11.	8.8+0.00016i	11.-0.0027i		
$T_{\bar{K}D_s^*}^{(1/2)}$	0.46	0.51	0.31	0.42	3.6+8.3i	1.1+4.4i	4.+8.3i	1.5+4.4i		
$T_{\eta D^*}^{(1/2)}$	0.14+0.0021i	0.16	0.088+0.0018i	0.13	0.32+3.i	-2.9+1.6i	0.46+3.i	-2.8+1.6i		
$T_{\eta D_s^*}^{(0)}$	-0.022	0.013	-0.015	0.016	0.025+6.1i	-6.2+3.2i	0.0036+6.1i	-6.2+3.2i		

for these channels. From Table I, we see that the chiral expansion of the pion channels converges well. The loop diagrams contribute largely to the kaon and eta channels due to the large mass of kaon and eta. But luckily they are cancelled by the tree diagram at  $O(\epsilon^3)$ , which makes the whole result convergent.

We compare the loop contribution between the HM $\chi$ PT and IR scheme in Table II. For both cases the dominant loop contributions are those with the intermediate state  $D^*$  meson. The numerical results are similar in the pion-scattering channels with these two different schemes. But the results differ greatly in the eta scattering channels.

The mass difference  $\delta$  affects our results only through the intermediate  $D$  meson in the loop diagrams. For comparison, we list the  $\delta$ -dependent part of the  $T$ -matrices in Table II when  $\delta \rightarrow 0$  and  $\delta = 142$  MeV. We notice that the correction from the heavy quark symmetry breaking in the loop diagrams with the  $D$  meson intermediate state is small in the  $KD^*$  channels. However, such a correction is significant in the  $\pi D^{*I=3/2}$ ,  $\pi D^{*I=1/2}$  and  $\eta D_s^{*I=0}$  channels.

From Table II, the IR scheme lowers the loop contribution in the channels  $T_{\pi D^*}^{(3/2)}$ ,  $T_{\pi D^*}^{(1/2)}$ ,  $T_{\pi D_s^*}^{(1)}$ ,  $T_{KD^*}^{(0)}$ , and  $T_{\bar{K}D_s^*}^{(1/2)}$ . The  $T$ -matrices of the  $\phi D$  scattering in the nonrelativistic  $\chi$ PT were compared with those in the relativistic  $\chi$ PT with the extended-on-mass-shell renormalization schemes in Ref. [20]. The relativistic effect would also lower the loop contribution in some channels such as  $T_{\pi D}^{(3/2)}$ ,  $T_{\pi D}^{(1/2)}$ .

The resonance  $D_{s1}(2460)$  couples to the  $D^*K$  strongly. Its role is similar to that of  $\Delta(1232)$  in the case of the pion nucleon scattering.  $D_{s1}(2460)$  is very close to the  $D^*K$  threshold and may be quite important for the  $D^*K$   $T$ -matrix. In contrast, the non-strange P-wave axial-vector  $D$  meson lies well above the  $D^*\pi$  threshold. Its contribution is less important. In this work we have tried to include some of the corrections from the P-wave axial-vector  $D$  meson through the LEC  $c_3$ . We expect that the results would be improved particularly for the  $D^*K$  channel if  $D_{s1}(2460)$  is



TABLE III: The threshold  $T$ -matrices for the pseudoscalar meson and  $\bar{B}^*$  meson scattering order by order in units of fm with HM $\chi$ PT.

	$O(\epsilon^1)$ $O(\epsilon^2)$		$O(\epsilon^3)$			Total	Scattering length
			loop	tree	total		
$T_{\pi\bar{B}^*}^{(3/2)}$	-3.2	0.44	-1	0.17	-0.83	-3.6	-0.14
$T_{\pi\bar{B}^*}^{(1/2)}$	6.5	0.44	0.58	-0.33	0.24	7.1	0.28
$T_{\pi\bar{B}_s^*}^{(1)}$	0	0.063	-1.1	0	-1.1	-1	-0.04
$T_{K\bar{B}^*}^{(0)}$	15	6.9	11	-9.8	0.72	23	0.83
$T_{K\bar{B}^*}^{(1)}$	0	0.53	-1.4+5.6 <i>i</i>	0	-1.4+5.6 <i>i</i>	-0.88+5.6 <i>i</i>	-0.032+0.2 <i>i</i>
$T_{K\bar{B}_s^*}^{(1/2)}$	-7.6	3.7	-6.2	4.9	-1.3	-5.2	-0.19
$T_{K\bar{B}^*}^{(1)}$	-7.6	3.7	-7.6	4.9	-2.7	-6.6	-0.24
$T_{K\bar{B}^*}^{(0)}$	7.6	-2.6	9.1	-4.9	4.2	9.2	0.34
$T_{K\bar{B}_s^*}^{(1/2)}$	7.6	3.7	3.7+8.3 <i>i</i>	-4.9	-1.2+8.3 <i>i</i>	10.+8.3 <i>i</i>	0.37+0.3 <i>i</i>
$T_{\eta\bar{B}^*}^{(1/2)}$	0	1	0.37+3. <i>i</i>	0	0.37+3. <i>i</i>	1.4+3. <i>i</i>	0.049+0.11 <i>i</i>
$T_{\eta\bar{B}_s^*}^{(0)}$	0	5.2	0.022+6.1 <i>i</i>	0	0.022+6.1 <i>i</i>	5.2+6.1 <i>i</i>	0.19+0.22 <i>i</i>

included as an explicit degree of freedom as  $\Delta(1232)$  in heavy baryon chiral perturbation theory [39–41].

We can also study the pseudoscalar meson and  $\bar{B}^*$  meson scattering with  $P_\mu^*$  and  $P$  representing  $(B^-, \bar{B}^0, \bar{B}_s^0)$  and  $(B^{*-}, \bar{B}^{*0}, \bar{B}_s^{*0})$ , respectively, in Eq. (4). The situation is very similar to the  $D^*$  case. With the following different constants

$$c_0 = 0.08 \text{ GeV}^{-1}, \quad c_1 = 0.10 \text{ GeV}^{-1}, \quad c_2 = -0.25 \text{ GeV}^{-1}, \quad c_3 = 0.44 \text{ GeV}^{-1},$$

$$\kappa^r = -0.33 \text{ GeV}^{-2}, \quad \bar{M} = 5323 \text{ MeV}, \quad \delta = 46 \text{ MeV}, \quad (36)$$

and  $g = 0.52$  [42], we can also analyze the interaction of the pseudoscalar meson and  $\bar{B}^*$  meson. The numerical results with HM $\chi$ PT are shown in Table III. They are only slightly different from those of the pseudoscalar meson and  $D^*$  meson scattering.

As mentioned in Ref [18], it is easy to get pseudoscalar meson and heavy antimeson scattering lengths with the C-parity transformation,

$$T_{H\bar{K}}^{(I)} = T_{H\bar{K}}^{(I)}, \quad T_{\bar{H}K}^{(I)} = T_{H\bar{K}}^{(I)}, \quad T_{H\pi/\eta}^{(I)} = T_{H\pi/\eta}^{(I)}, \quad (37)$$

where  $I$  is the total isospin and  $H(\bar{H})$  denotes the heavy meson(antimeson).

In short, we have investigated the pseudoscalar meson and  $D^*$  meson scattering lengths to  $O(\epsilon^3)$  with HM $\chi$ PT and IR methods. The chiral expansion in the  $\pi D^*$  channels converges well. We hope our present study may be helpful to the possible extrapolation in the future lattice simulation of the light meson and heavy meson scattering. Our results may also be useful to the phenomenological investigation of the possible molecular states composed of one heavy meson and one light meson.

### Acknowledgments

YRL thanks L.S. Geng for communications about results in Ref. [18]. This project is supported by the National Natural Science Foundation of China under Grants No. 11075004, No. 11021092, No. 11035006, No. 11047606, No. 10805048, and the Ministry of Science and Technology of China (No. 2009CB825200), and the Ministry of Education of China (FANEDD under Grants No. 200924, DPFIE under Grants No. 20090211120029, NCET under Grants No. NCET-10-0442, the Fundamental Research Funds for the Central Universities under Grants No. lzujbky-2010-69). YRL was partially supported by JSPS KAKENHI (21.09027).

### Appendix A: The uncertainty of LECs with resonance saturation method

Other resonances with the same quantum numbers as  $\sigma$ ,  $\kappa$ , and  $D_{s1}(2460)$  will also contribute to  $c_i$ 's. Generally, the heavier the resonance is, the less its contribution to the LECs. Here we will check the uncertainty which other resonances would cause.

From Eq. (29), we see that  $\sigma$  does not contribute to  $c_1$  and  $c_3$ . For the LECs  $c_0$  and  $c_2$ , the contribution  $\mathcal{K}$  from the  $\sigma$  and  $\kappa$  scales as

$$\frac{|\mathcal{K}_\kappa|}{|\mathcal{K}_\sigma|} = \frac{m_\sigma^2}{m_\kappa^2} = 0.3. \quad (\text{A1})$$

In principle the LECs would absorb the contributions from the  $f_0(1370)$  singlet and the  $K_0^*$  octet ( $K_0^*(1430)$ ,  $a_0(1450)$ ,  $f_0(1500)$ ) and other heavier resonances similarly. Similar to Eq. (A1),

$$\frac{|\mathcal{K}_{f_0(1370)}|}{|\mathcal{K}_{K_0^*}|} = \frac{m_{f_0(1370)}^2}{m_{K_0^*}^2} = 0.9. \quad (\text{A2})$$

In the channel  $f_0(1500) \rightarrow \eta\eta$  and  $f_0(1500) \rightarrow K\bar{K}$ , the decay momentum is 516 and 568 MeV respectively. We can estimate the magnitude of  $c_{d,K_0^*}$  and  $c_{m,K_0^*}$  using the experimental partial width

$$\Gamma(f_0(1500) \rightarrow \eta\eta) = 109_{-7}^{+7} \times (5.1_{-0.9}^{+0.9})\% \text{ MeV}, \quad \Gamma(f_0(1500) \rightarrow K\bar{K}) = 109_{-7}^{+7} \times (8.6_{-1.0}^{+1.0})\% \text{ MeV}, \quad (\text{A3})$$

and similar effective Lagrangians as in Eq. (26). One gets

$$\begin{cases} |c_{d,K_0^*}| \sim 1.9 \times 10^{-2} \text{ GeV}, & |c_{m,K_0^*}| \sim 3.0 \times 10^{-2} \text{ GeV}, & c_{d,K_0^*} c_{m,K_0^*} < 0; \\ |c_{d,K_0^*}| \sim 1.3 \times 10^{-2} \text{ GeV}, & |c_{m,K_0^*}| \sim 1.5 \times 10^{-2} \text{ GeV}, & c_{d,K_0^*} c_{m,K_0^*} > 0. \end{cases} \quad \text{or} \quad (\text{A4})$$

Therefore,

$$\frac{|\mathcal{K}_{K_0^*}|}{|\mathcal{K}_\kappa|} = \frac{|c_{d/m,K_0^*}|}{|c_{d/m}|} \frac{|c_{K_0^*}|}{|c_\kappa|} \frac{m_\kappa^2}{m_{K_0^*}^2} \lesssim \frac{|c_{K_0^*}|}{|c_\kappa|} \frac{m_\kappa^2}{m_{K_0^*}^2} = 0.3 \frac{|c_{K_0^*}|}{|c_\kappa|} \sim 0.3, \quad (\text{A5})$$

In the last step we have assumed that the coupling  $c_{K_0^*}$  in the  $D^*D^*K_0^*$  vertex is of the same order as  $c_\kappa$ . Now we have  $|\mathcal{K}_{K_0^*}| \sim 0.3 |\mathcal{K}_\kappa|$  and  $|\mathcal{K}_{f_0(1370)}| \sim 0.1 |\mathcal{K}_\sigma|$ . In other words, the  $c_i$ 's' correction from the heavier resonances is roughly 30%.

In principle, heavy vector resonances  $D_1(2420)(D_{s1}(2536))$  would also give corrections to  $c_3$ ,

$$\Delta c_3 = \frac{|G_1 + G_2|_{D_1(2420)}^2 M_{D^*}}{2(M_{D_1(2420)}^2 - M_{D^*}^2)}. \quad (\text{A6})$$

By fitting  $\Gamma(D_{s1}(2536) \rightarrow D^*K) < \Gamma(D_{s1}(2536)) < 2.3 \text{ MeV}$ , one finds  $|G_1 + G_2|_{D_1(2420)} < 0.16$ . So  $|\Delta c_3| < 0.03 \text{ GeV}^{-1}$ , which is less than 10% of  $c_3$  in Eq. (34).

Moreover, the variation of the mass of the  $\kappa$  octet from 658 MeV to 985 MeV would introduce the 20% uncertainty to  $c_0$  and  $c_2$  and 60% uncertainty to  $c_1$  and  $c_3$ . In short, the determination of  $c_i$ 's in Eq.(34) are not accurate. But their sign and order of magnitude should be reliable.

## Appendix B: Some functions and constants in the infrared scheme

We perform the tensor decomposition of the IR integrals as follows,

$$\begin{aligned} & \frac{1}{i} \int_I \frac{d^d k}{(2\pi)^d} \frac{\{1, k^\mu, k^\mu k^\nu\}}{(k^2 - m^2 + i\epsilon) [(p-k)^2 - M^2 + i\epsilon]} \\ &= \{I^{(0)}(p^2, m^2, M^2), \quad p^\mu I^{(1)}(p^2, m^2, M^2), \quad g^{\mu\nu} I^{(2)}(p^2, m^2, M^2) + p^\mu p^\nu I^{(3)}(p^2, m^2, M^2)\}, \end{aligned} \quad (\text{B1})$$

$$\begin{aligned} & \frac{1}{i} \int_I \frac{d^d k}{(2\pi)^d} \frac{\{1, k^\mu, k^\mu k^\nu, k^\mu k^\nu k^\rho\}}{(k^2 - m_1^2 + i\epsilon)(k^2 - m_2^2 + i\epsilon) [(p-k)^2 - M^2 + i\epsilon]} \\ &= \{F_0(p^2, m_1^2, m_2^2, M^2), \quad p^\mu F_1(p^2, m_1^2, m_2^2, M^2), \quad g^{\mu\nu} F_2(p^2, m_1^2, m_2^2, M^2) + p^\mu p^\nu F_3(p^2, m_1^2, m_2^2, M^2), \\ & \quad p^\mu p^\nu p^\rho F_4(p^2, m_1^2, m_2^2, M^2) + (g^{\mu\nu} p^\rho + g^{\mu\rho} p^\nu + g^{\nu\rho} p^\mu) F_5(p^2, m_1^2, m_2^2, M^2)\}, \end{aligned} \quad (\text{B2})$$

where  $M$  is the mass of the heavy meson and  $m, m_1, m_2$  are the masses of the light pseudoscalar mesons. The Lorentz invariant coefficient  $I^{(0)}$  can be written as [25],

$$I^{(0)}(p^2, m^2, M^2) = -\frac{p^2 - M^2 + m^2}{p^2} L - \frac{1}{32\pi^2} \frac{p^2 - M^2 + m^2}{p^2} (2 \log \frac{m}{\lambda} - 1)$$

$$+ \frac{\alpha}{8\pi^2 \tilde{\omega}^2} \times \begin{cases} -\sqrt{1-\Omega^2} \cos^{-1}\left(-\frac{\Omega+\alpha}{\tilde{\omega}}\right) & |\Omega| \leq 1 \\ \sqrt{\Omega^2-1} \log\left(\sqrt{\left(\frac{\Omega+\alpha}{\tilde{\omega}}\right)^2-1} - \frac{\Omega+\alpha}{\tilde{\omega}}\right) & \Omega < -1, \\ \sqrt{\Omega^2-1} \left\{ i\pi + \log\left(\frac{\Omega+\alpha}{\tilde{\omega}} - \sqrt{\left(\frac{\Omega+\alpha}{\tilde{\omega}}\right)^2-1}\right) \right\} & \Omega > 1 \end{cases}, \quad (\text{B3})$$

where

$$\Omega = \frac{p^2 - m^2 - M^2}{2Mm}, \quad \alpha = \frac{m}{M}, \quad \tilde{\omega} = \sqrt{1 + 2\alpha\Omega + \alpha^2}, \quad L = \frac{\lambda^{D-4}}{16\pi^2} \left\{ \frac{1}{D-4} + \frac{1}{2}(\gamma_E - 1 - \ln 4\pi) \right\}. \quad (\text{B4})$$

The other coefficients are

$$\begin{aligned} I^{(1)}(p^2, m^2, M^2) &= \frac{p^2 - M^2 + m^2}{2p^2} I^{(0)}(p^2, m^2, M^2) + \frac{m^2}{p^2} \left( L + \frac{1}{16\pi^2} \log \frac{m}{\lambda} \right), \\ I^{(2)}(p^2, m^2, M^2) &= \frac{1}{d-1} \left( m^2 I^{(0)}(p^2, m^2, M^2) - \frac{p^2 - M^2 + m^2}{2} I^{(1)}(p^2, m^2, M^2) \right), \\ I^{(3)}(p^2, m^2, M^2) &= \frac{p^2 - M^2 + m^2}{2p^2} I^{(1)}(p^2, m^2, M^2) - \frac{1}{p^2} I^{(2)}(p^2, m^2, M^2), \\ F_j(p^2, m_1^2, m_2^2, M^2) &= \frac{I^{(j)}(p^2, m_1^2, M^2) - I^{(j)}(p^2, m_2^2, M^2)}{m_1^2 - m_2^2}, \quad j = 0, 1, 2, 3, \\ F_4(p^2, m_1^2, m_2^2, M^2) &= \frac{1}{p^2 d} \left( \frac{d+2}{2} I^{(3)}(p^2, m_2^2, M^2) + \frac{d+2}{2} (p^2 - M^2 + m_1^2) F_3(p^2, m_1^2, m_2^2, M^2) \right. \\ &\quad \left. - 2I^{(1)}(p^2, m_2^2, M^2) - 2m_1^2 F_1(p^2, m_1^2, m_2^2, M^2) \right), \\ F_5(p^2, m_1^2, m_2^2, M^2) &= \frac{1}{4} I^{(3)}(p^2, m_2^2, M^2) + \frac{p^2 - M^2 + m_1^2}{4} F_3(p^2, m_1^2, m_2^2, M^2) - \frac{p^2}{2} F_4(p^2, m_1^2, m_2^2, M^2). \end{aligned} \quad (\text{B5})$$

With the definitions,

$$\begin{aligned} h_1(m) &\equiv \frac{g^2 \{ 2M_D^2 F_5(M_{D^*}^2, m^2, m^2, M_D^2) + 4M_{D^*}^2 F_5(M_{D^*}^2, m^2, m^2, M_{D^*}^2) \}}{f^4}, \\ h_2(m) &\equiv \frac{g^2 M_D^2}{f^4 M_{D^*}} \partial_x I^{(2)}(x^2, m^2, M_D^2)|_{x \rightarrow M_{D^*}} + \frac{2g^2 M_{D^*}}{f^4} \partial_x I^{(2)}(x^2, m^2, M_{D^*}^2)|_{x \rightarrow M_{D^*}}, \\ h_3(m) &\equiv \frac{g^2 M_D}{f^4} \partial_x I^{(2)}(M_{D^*}^2, m^2, x^2)|_{x \rightarrow M_D} + \frac{2g^2 M_{D^*}}{f^4} \partial_x I^{(2)}(M_{D^*}^2, m^2, x^2)|_{x \rightarrow M_{D^*}}, \end{aligned} \quad (\text{B6})$$

we can show the functions used for IR in Eq. (17),

$$\begin{aligned} W(m) &= \frac{g^2}{f^4} \{ 4M_{D^*} F_2(M_{D^*}, m, m, M_{D^*}) + 2M_D F_2(M_{D^*}, m, m, M_D) \}_r, \\ J &= \frac{g^2}{f^4} \{ 4M_{D^*} F_2(M_{D^*}, m_\eta, m_\pi, M_{D^*}) + 2M_D F_2(M_{D^*}, m_\eta, m_\pi, M_D) \}_r, \\ V(m, \omega) &= \frac{3m^2 \omega}{8\pi^2 f^4} \log \frac{m}{\lambda} - \frac{1}{f^4} \left\{ 2M_{D^*} \omega^2 I^{(0)}(\omega + M_{D^*}, m, M_{D^*}) + 4M_{D^*}^2 \omega I^{(1)}(\omega + M_{D^*}, m, M_{D^*}) \right. \\ &\quad \left. + 2M_{D^*} I^{(2)}(\omega + M_{D^*}, m, M_{D^*}) + 2M_{D^*}^3 I^{(3)}(\omega + M_{D^*}, m, M_{D^*}) \right\}_r, \\ V_1 &= m_\pi \left\{ -\frac{1}{2} h_1(m_K) - h_1(m_\pi) - \frac{3}{4} h_2(m_\pi) - \frac{1}{2} h_2(m_K) - \frac{1}{12} h_2(m_\eta) + \frac{1}{4} h_3(m_\pi) - \frac{1}{12} h_3(m_\eta) \right\}_r, \\ V_2 &= m_K \left\{ -h_1(m_K) - \frac{2}{3} h_2(m_K) - \frac{2}{9} h_2(m_\eta) + \frac{1}{3} h_3(m_K) - \frac{2}{9} h_3(m_\eta) \right\}_r, \\ V_3 &= m_K \left\{ -h_1(m_\pi) - \frac{1}{2} h_2(m_\pi) - \frac{1}{3} h_2(m_K) - \frac{1}{18} h_2(m_\eta) + \frac{1}{2} h_3(m_\pi) - \frac{1}{3} h_3(m_K) - \frac{1}{18} h_3(m_\eta) \right\}_r, \\ V_4 &= m_K \left\{ \frac{3}{2} h_2(m_\pi) - h_2(m_K) - \frac{1}{2} h_2(m_\eta) + \frac{3}{2} h_3(m_\pi) - h_3(m_K) - \frac{1}{2} h_3(m_\eta) \right\}_r. \end{aligned} \quad (\text{B7})$$

The  $\{X\}_r$  in Eq. (B7) represents  $\lim_{d \rightarrow 4} X$  after removing the terms proportional to  $L$ .

- 
- [1] I. Adachi *et al.* [Belle Collaboration], arXiv:1105.4583 [hep-ex].
  - [2] E. van Beveren and G. Rupp, Phys. Rev. Lett **91**, 012003 (2003).
  - [3] Y. Dai, X. Li, Shi-Lin Zhu, and Y. Zuo, Eur. Phys. J. C **55**, 249 (2008).
  - [4] J. Flynn and J. Nieves, Phys. Rev. D **75**, 074024 (2007).
  - [5] S. Aoki, T. Hatsuda, and N. Ishii, Prog. Theor. Phys. **123**, 89 (2010).
  - [6] A. Torok, *et al.*, Phys. Rev. D **81**, 074506 (2010).
  - [7] M. Gong, *et al.*, arXiv:1103.0589v2 [hep-lat] (2011).
  - [8] S. Dong, *et al.*, arXiv:0911.0868 (2009).
  - [9] C. Bernard, *et al.*, Phys. Rev. D **65**, 014510 (2001).
  - [10] C.-H. Lee, H. Jung, D.-P. Min, and M. Rho, Phys. Lett. B **326**, 14 (1994).
  - [11] M. Mojzis, Eur. Phys. J. C **2**, 181 (1998).
  - [12] N. Kaiser, Phys. Rev. C **64**, 045204 (2001).
  - [13] T. D. Cohen and R. F. Lebed, Phys. Rev. D **74**, 056006 (2006).
  - [14] G.-Z. Meng, *et al.*, Phys. Rev. D **80**, 034503 (2009).
  - [15] D. Gamermann, E. Oset, D. Strottman, and M. J. V. Vacas, Phys. Rev. D **76**, 074016 (2007).
  - [16] A. Torok, *et al.*, Phys. Rev. D **81**, 074506 (2010).
  - [17] S. Scherer, Adv. Nucl. Phys. **27**, 277 (2003).
  - [18] Y.-R. Liu, X. Liu, and Shi-Lin Zhu, Phys. Rev. D **79**, 094026 (2009).
  - [19] F. Guo, C. Hanhart, and U. Meißner, Eur. Phys. J. A **40**, 171 (2009).
  - [20] L. Geng, N. Kaiser, J. Martin-Camalich, and W. Weise, Phys. Rev. D **82**, 54022 (2010).
  - [21] T.-M. Yan, *et al.*, Phys. Rev. D **46**, 1148 (1992).
  - [22] P. Cho, Nucl. Phys. B **396**, 183 (1993).
  - [23] M. B. Wise, Phys. Rev. D **45**, R2188 (1992).
  - [24] R. Casalbuoni, *et al.*, Phys. Rep. **281**, 145 (1997).
  - [25] T. Becher and H. Leutwyler, Eur. Phys. J. C **9**, 643 (1999).
  - [26] T. Becher and H. Leutwyler, JHEP **0106**, 017 (2001).
  - [27] B. Kubis and U.-G. Meißner, Nucl. Phys. A **679**, 698 (2001).
  - [28] Shi-Lin Zhu, S. Puglia, and M. J. Ramsey-Musolf, Phys. Rev. D **63**, 034002 (2001).
  - [29] J. Gasser and H. Leutwyler, Nucl. Phys. B **250**, 465 (1985).
  - [30] Z.-W. Liu, Y.-R. Liu, and Shi-Lin Zhu, Phys. Rev. D **83**, 034004 (2011).
  - [31] K. Nakamura and *et al.*, J. Phys. G **37**, 075021 (2010).
  - [32] G. Ecker, J. Gasser, A. Pich, and E. D. Rafael, Nucl. Phys. B **321**, 311 (1989).
  - [33] V. Bernard, N. Kaiser, and U.-G. Meißner, Phys. Lett. B **309**, 421 (1993).
  - [34] P. Colangelo and F. De Fazio, Eur. Phys. J. C **4**, 503 (1998).
  - [35] I. Caprini, G. Colangelo, and H. Leutwyler, Phys. Rev. Lett **96**, 132001 (2006).
  - [36] S. Descotes-Genon and B. Moussallam, Eur. Phys. J. C **48**, 553 (2006).
  - [37] L. Liu, H. Lin, and K. Orginos, arXiv:0810.5412 [hep-lat] (2008).
  - [38] Y.-R. Liu and Shi-Lin Zhu, Phys. Rev. D **75**, 034003 (2007).
  - [39] E. Jenkins and A. V. Manohar, Phys. Lett. B **259**, 353 (1991).
  - [40] T. R. Hemmert, B. R. Holstein, and J. Kambor, J. Phys. G: Nucl. Part. Phys. **24**, 1831 (1998).
  - [41] Y.-R. Liu and Shi-Lin Zhu, Eur. Phys. J. C **52**, 177 (2007).
  - [42] H. Ohki, H. Matsufuru, and T. Onogi, Phys. Rev. D **77**, 094509 (2008).